Journal of Luminescence 169 (2016) 838–843

Contents lists available at ScienceDirect

Journal of Luminescence

journal homepage: www.elsevier.com/locate/jlumin

On the synthesis of LuAG:Ce fine powders by molten salts methods and spectroscopic properties of the products

Ioannis E. Seferis [a], Eugeniusz Zych [a,b,*]

[a] Faculty of Chemistry, University of Wroclaw, 14. F. Joliot-Curie Street, 50-383 Wroclaw, Poland
[b] Wroclaw Research Centre EIT+, 147 Stablowicka Street, 54-066 Wroclaw, Poland

ARTICLE INFO

Article history:
Received 12 December 2014
Accepted 24 January 2015
Available online 2 February 2015

Keywords:
LuAG:Ce
Molten salts synthesis
Photoluminescence
Luminescence kinetics

ABSTRACT

$Lu_3Al_5O_{12}$:Ce (LuAG:Ce) powders were synthesized at temperatures as low as 450–550 °C by means of a molten salts technique with eutectic mixtures of $NaNO_2$ and KNO_2 or $NaNO_2$, KNO_2 and Na_2CO_3. Addition of sodium carbonate allowed getting phase pure cubic LuAG:Ce even at 450 °C while without it the needed temperature was 500 °C. The powders had well defined morphology with particles sizes reaching 200–250 nm or 150–250 nm when Na_2CO_3 was used. The spectroscopic properties of the materials were characterized in the 17–700 K range of temperatures. The ratio of the two Ce^{3+} related excitation bands located at 345 and 450 nm were found to increase significantly between 17 K and 350 K while above that range of temperatures it was quite constant. This ratio was shown to vary strongly depending on the atmosphere of synthesis. Heating at 1150 °C in air reduced the efficiency of the excitation into the 345 nm very significantly, which was ascribed to formation of defects, among them also appearance of Ce^{4+}, whose competing absorption overlapping the 345 nm excitation band effectively reduced its contribution to the luminescence compared to the 450 nm band. Decay times were pretty constant in the 17–300 K range of temperatures and also were independent on the atmosphere of post-fabrication heat-treatment.

1. Introduction

Synthesis of new phosphor materials as well as the old ones by means of new methods is ubiquitous as a result of the requirements of next generation high-performance applications. Lutetium based scintillators and X-ray phosphors attracts great attention due to their high density and high effective *Z*-number, which assures high stopping power for ionizing radiation quanta [1,2].

Lutetium aluminum garnet, $Lu_3Al_5O_{12}$ (LuAG) has higher density (6.7 g/cm^3) and higher *Z* number (63) compared to the isostructural $Y_3Al_5O_{12}$ (YAG). This results in higher overall absorption and stopping power for X- and γ-rays. Ce activated LuAG has been investigated in the form of single crystal screens for high resolution X-ray imaging application with very promising results [3]. LuAG:Ce single crystal has also been considered as potential candidate to replace BGO in PET scanners due to the six times shorter decay time and almost identical density [4]. Interestingly, its rather high refractive index (1.85 at 520 nm) enhances scattering by the powder phosphor particles, and this is advantageous in terms of mixing the exciting blue light from the semiconductor light emitting diode (LED) with the yellow photons emitted by the phosphor particles [5].

On the other hand, from the aspect of luminescence efficiency the LuAG:Ce appeared troublesome. A rather small misfit of the Lu and Al ionic radii (0.861 Å vs. 0.535 Å) makes the LuAG:Ce prone to incorporate antisite defects even easier than YAG:Ce [6]. For this reason the constraint of anti-site defects population and the resulting structural disorder they cause is of interest. Since these defects appear mostly as a result of high-temperature treatment, development of fabrication techniques of good quality LuAG:Ce at reduced temperatures is important. The anti-site defects are blamed for afterglow in LuAG:Ce as well as reduced emission efficiency due to generation of nonradiative pathways of energy dissipation [6,7].

In this paper we report on making fully crystalline LuAG:Ce at temperatures as low as 450–550 °C. The synthesis is based on the molten salts method, which we previously successfully applied for making YAG:Ce [8]. The structure and morphology of the products synthesized with two different compositions of the molten salts will be analyzed by an X-ray powder diffraction and scanning electron microscopy. Photoluminescencent properties of raw and additionally annealed in different atmospheres (air, vacuum and H_2–N_2) powders will be presented at 17–700 K range of temperatures.

* Corresponding author at: Faculty of Chemistry, University of Wroclaw, 14. F. Joliot-Curie Street, 50-383 Wroclaw, Poland.
E-mail address: eugeniusz.zych@chem.uni.wroc.pl (E. Zych).

http://dx.doi.org/10.1016/j.jlumin.2015.01.051
0022-2313/

2. Materials synthesis and experimental procedures

For the synthesis of LuAG:Ce by the molten salts method, $Lu(NO_2)_3$ $6H_2O$, $Al(NO_2)_3$ $9H_2O$, and $Ce(NO_2)_3$ $6H_2O$ were used as starting materials. The formal Ce concentration varied within 1–5% with respect to Lu. The nitrates were thoroughly mixed with starting composition and added to one of the two used eutectic mixtures of molten salts. The first eutectic mixture consisted of 65% $NaNO_2$ and 35% KNO_2, while the other contained additionally 5% of Na_2CO_3 to make the flux more alkaline. The blend of nitrates was mixed with an eutectic mixture at a mass ratio 7:10 in a platinum crucible, which was then transferred to a furnace and heated at 450 °C, 500 °C and 550 °C for 5 h. After cooling, the raw LuAG:Ce material was recovered by washing with water and drying at 60 °C in air overnight. In each case a part of the raw powder was additionally heat-treated at 1150 °C for 1 h, in air, vacuum or in forming gas containing 25% of H_2.

The X-ray powder diffraction measurements were performed on a Bruker D8 Advance X-ray diffractometer, using CuKα_1 (1.54056A) radiation, in the range of $2\theta=10–100^\circ$ with the step of $2\theta=0.024^\circ$. The morphology of the powders was determined by Hitachi S-3400 N Scanning Electron Microscope (SEM) equipped with energy dispersive X-ray spectroscopy (EDAX) analyzer. Photoluminescence excitation and emission spectra measurements were performed with FLS 980 Spectrofluorimeter from Edinburgh Instruments (Livingstone, UK) equipped with a 450 W continuous Xe lamp, and S900 photomultiplier detector operating within 180–870 nm. Decay traces were taken with the same FLS 980 Spectrofluorimeter and Supercontinuum Fianium laser with the pulse duration of 6 ps and repetition rate of 40 MHz.

3. Results

Fig. 1a and b shows XRD patterns of the powders prepared using the two different fluxes, $NaNO_2+KNO_2$ (Fig. 1a) and $NaNO_2+KNO_2+Na_2CO_3$ (Fig. 1b), at different temperatures synthesis from 450 to 550 °C and post-treated at 1150 °C. Fig. 1c shows XRD patterns of LuAG:*x*% Ce ($x=1–5$) powders prepared with the use of $NaNO_2+KNO_2+Na_2CO_3$ flux, at 550 °C and post-treated at 1150 °C. Fig. 1d shows exemplary XRD patterns measured for raw powders without any additional heat-treatments and these diffractograms prove that already such powders possess the cubic structure of LuAG. For comparison a simulated pattern of cubic LuAG is given in each of the figures. From Fig. 1a and b it is obvious that each synthesis led to cubic LuAG. Yet, using the $NaNO_2+KNO_2$ flux at 450 °C some unreacted Lu_2O_3 was detected as admixture to LuAG. The more

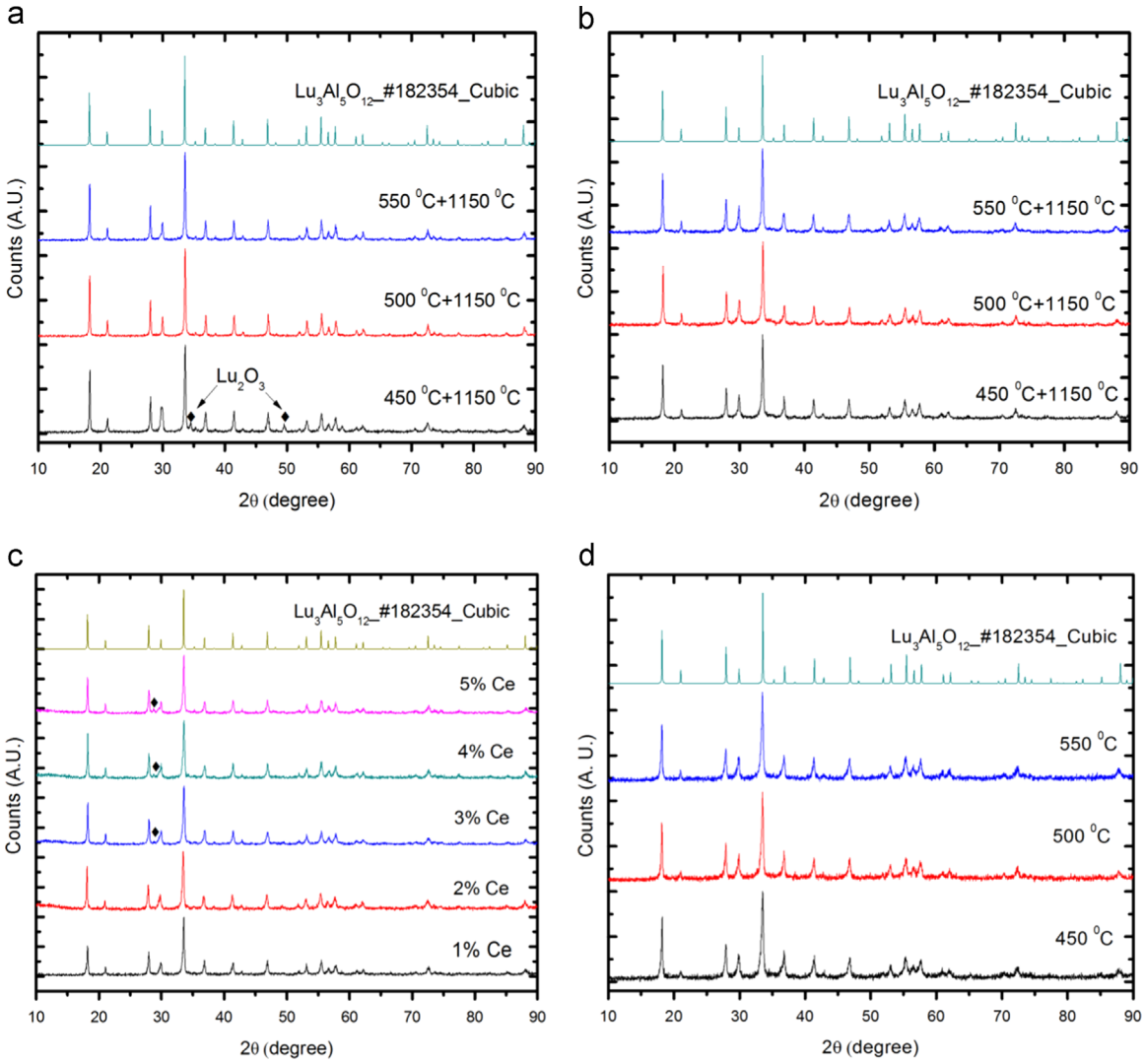

Fig. 1. (a) XRD patterns of LuAG:1% Ce synthesized with $NaNO_2+KNO_2$ flux at 450, 500 and 550 °C and post-treated at 1150 °C. (b) XRD patterns of LuAG:1% Ce synthesized with $NaNO_2+KNO_2+Na_2CO_3$ flux at 450, 500 and 550 °C and post-treated at 1150 °C. (c) XRD patterns of LuAG:*x*% Ce ($x=1$, 2, 3, 4, and 5) synthesized with $NaNO_2+KNO_2+Na_2CO_3$ flux at 550 °C and post-treated at 1150 °C. In c, ♦ denotes lines identified as resulting from CeO_2 traces.

alkaline flux containing Na_2CO_3 allowed getting phase pure LuAG even at 450 °C. Altogether, the XRDs prove that the molten salt technique is efficient in generation of cubic LuAG:Ce powders at extremely low temperatures. In Fig. 1c the recorded XRD patterns of the LuAG:Ce powders made at 550 °C and post-treated at 1150 °C for different Ce concentrations are given. As the Ce^{3+} concentrations increases above 2% there is observed a segregation of CeO_2 showing that Ce^{3+} has some difficulty to enter and dissolve in the LuAG host. This might be understood taking into account that in YAG:Ce sintered ceramics Ce was shown to significantly segregate at the grain boundary region [9]. This was clearly connected with the noticeably larger radius of Ce^{3+} ion (1.01 Å) compared to the Y^{3+} (0.9 Å) [10], which is being substituted. In the case of LuAG:Ce the difference is even higher, as Lu^{3+} radius is 0.861 Å [10]. Thus, it can be anticipated that in the case of nanocrystalline powders, a tendency of Ce to diffuse towards the surface of the grains must facilitate its precipitation as a separate phase, in our case CeO_2. Consequently, it cannot be excluded that even at low concentrations some Ce also separates as ceria instead of getting dissolved in the forming LuAG phase. An XRD technique is not sensitive enough to trace such tiny effects. Consequently, we expect that the real concentration of Ce in the LuAG:Ce powders obtained by the molten salts technique is lower than the formal one. We did not make precise analysis to find detailed numbers, however.

Fig. 2 shows the SEM images for the product synthesized with $NaNO_2+KNO_2$ flux (a, b, and c) and $NaNO_2+KNO_2+Na_2CO_3$ fluxes (d, e, and f) at temperatures of 450 °C (a and d) 500 °C (b and e) and 550 °C (c and f). All the presented images were taken after the post-fabrication heat-treatment at 1150 °C. Yet, the raw powders prepared at 450–550 °C have very similar morphology, so the additional heating did not lead to any noticeable mass transfer between the grains. The powders synthesized with $NaNO_2+KNO_2$ flux (a, b, and c) have narrow size distribution of about 200–250 nm and their shapes are almost spherical. Such characteristics are very desirable for some phosphor applications where screens with uniform phosphor layer are required. The powders synthesized with $NaNO_2+KNO_2+Na_2CO_3$ flux have broader, but still reasonable grain size distribution of about 150–250 nm. Agglomeration of grains is quite low in all the samples and should not have a negative influence on making homogeneous screens. The most uniform grains combined with the lowest agglomeration were achieved for the powder made with the $NaNO_2+KNO_2$ flux at 550 °C.

Fig. 3a and b shows the normalized excitation and emission spectra of Ce-doped LuAG powder annealed at 1150 °C in the reducing atmosphere of forming gas, measured in the 17–350 (3a) and in 350–700 K range of temperatures (3b). The excitation bands peaking near 345 nm and 450 nm represent transitions from the $4f^1$ ground state to the first, $5d_1$, and second, $5d_2$, excited 5d states of Ce^{3+}. At low temperatures the emission spectrum shows the well-known double band structure related to the transitions to the $^2F_{5/2}$ and $^2F_{7/2}$ spin–orbit states of the $4f^1$ electronic structure of Ce^{3+}. When the temperature gets higher the two emission bands broaden and their overlapping becomes continuously more significant and finally, above about 300–350 K, the doublet is no longer visible. Nevertheless, it is noteworthy that such characteristics of the Ce^{3+} luminescence proves that the dopant experiences well defined symmetry in the small crystallites of LuAG:Ce prepared at low temperatures.

Fig. 3 also reveals that the ratio of the excitation bands at 345 nm and 450 nm quite significantly varies between 17 and 350 K and is almost stable above 350 K. This is further proved in Fig. 4 showing the temperature dependence of the ratio of the oscillation strengths of the 345 and 450 nm $4f^1 \rightarrow 5d_1/5d_2$ excitation transitions (taken as the areas under the corresponding bands). Up to about 350 K the fraction continuously increases to become rather constant at yet higher temperatures. Similar observations were reported for YAG:Ce by Robbins [11] and were explained as resulting from thermally driven variations in occupancy of the Stark levels of the $2F_{5/2}$ state, which splits into two components, E″ and E′, due to some tetragonal distortion of the cubic Y^{3+} (Ce^{3+}) site. At lowest temperatures basically only the lowest Stark level, E″, is populated and thus excitation can start only from there. As the temperature increases, also the higher Stark level, E′, gets thermally populated and thus it may also serve as the starting level of excitation. Since among the $E'' \rightarrow 5d_2$ and

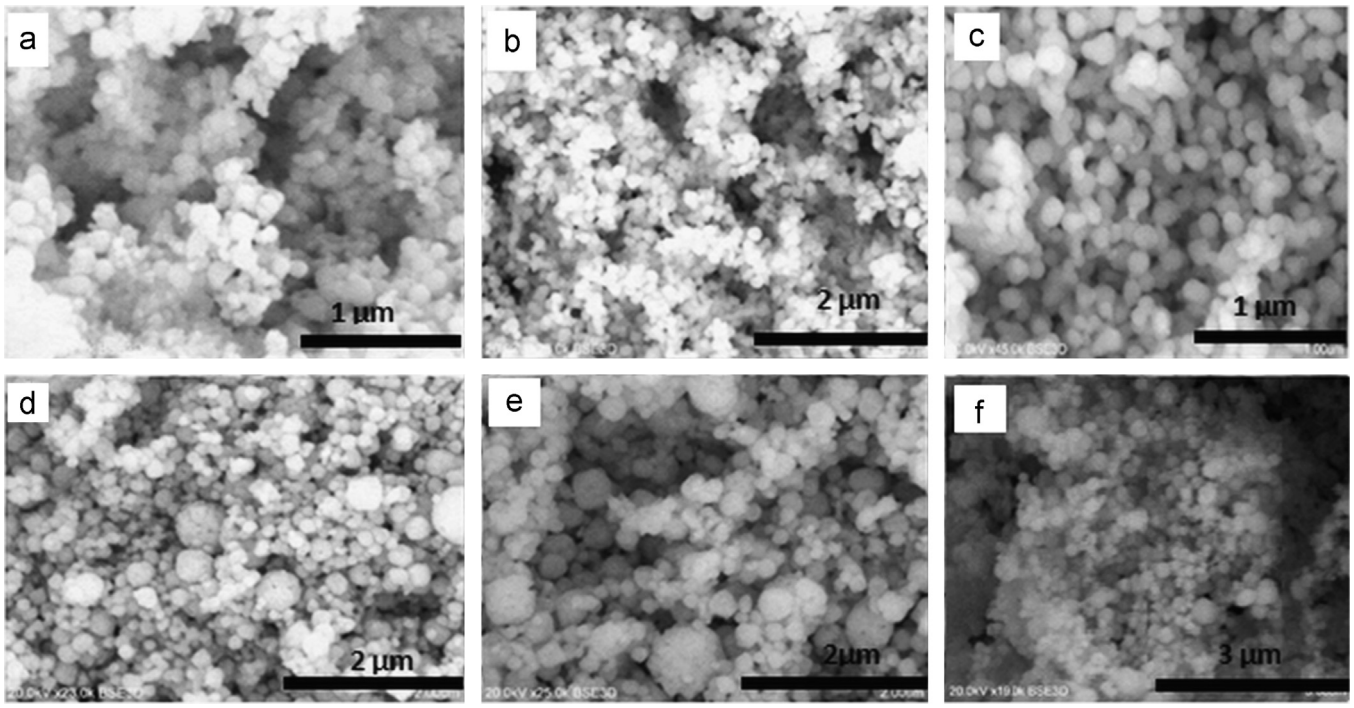

Fig. 2. SEM images for the products synthesized with $NaNO_2+KNO_2$ flux (a, b, and c) and $NaNO_2+KNO_2+Na_2CO_3$ flux (d, e, and f) at temperatures of 450 °C (a and d), 500 °C (b and e), and 550 °C (c and f). All samples were additionally heated at 1150 °C.

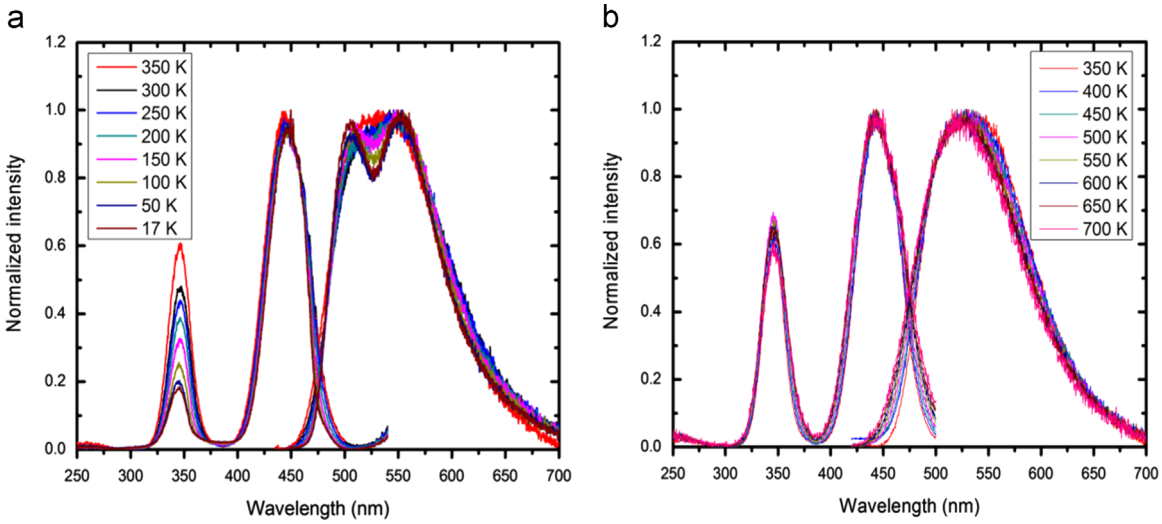

Fig. 3. Normalized excitation and emission spectra for Ce-doped LuAG, annealed at 1150 °C in air, measured at (a) low temperatures from 17 K to 300 K, and at (b) high temperatures from 350 K to 700 K.

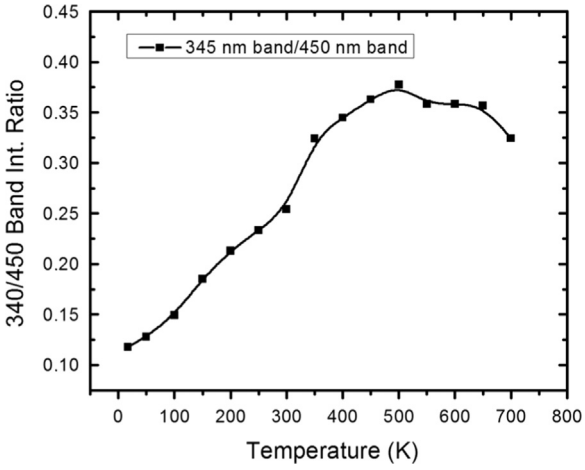

Fig. 4. The ratio of the 345 nm and 450 nm bands intensities as a function of temperature.

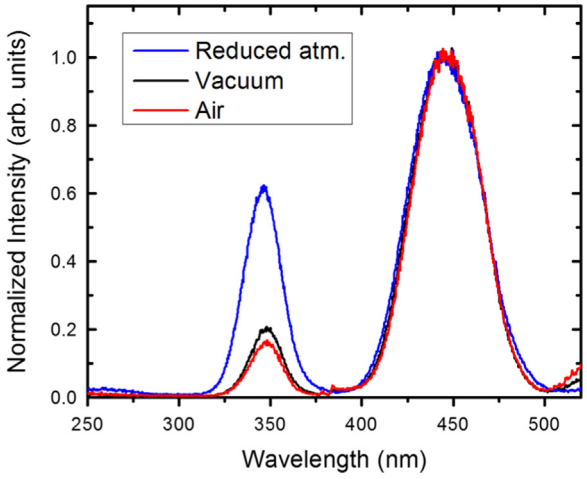

Fig. 5. Excitation spectra of 560 nm luminescence of the LuAG:Ce powders heat-treated at different atmospheres. Note the relative decrease of the 345 nm band intensity as the treatment atmosphere gets more oxidizing.

$E' \rightarrow 5d_2$ transitions contributing to the 345 nm excitation band the latter has much more allowed character the measured intensity of the 345 nm gets continuously higher with increasing temperature. Such variations in probabilities of the $E'' \rightarrow 5d_1$ and $E' \rightarrow 5d_1$ transitions do not occur [11] which leads to the observed temperature dependent ratio of intensities of the 345 nm and 450 nm excitation bands. Since this is exactly what is also observed in our LuAG:Ce fine powders the explanation should be analogous.

As seen in Fig. 5, the ratio of the 345 nm and 450 nm bands is also to a very significant extent affected by atmosphere of the post-fabrication treatment. This comparison we present only at RT. Clearly, as the atmosphere of treatment gets more oxidizing the band at 345 nm shows reduced intensity. A somewhat similar, though less profound, effect was reported for YAG:Ce sintered ceramics and was shown to be hardly observed for single crystals [12]. Yet, in Ref. [12] the decrease of excitation efficiency as short wavelengths in ceramics was found for yet more energetic components, below ~300 nm, which we are not able to access with our instrumentation. It was there justified that oxidizing atmosphere allowed to penetrate the material by Oxygen through grain boundaries and increase the population of defects mostly in the boundaries regions leading to a broad parasitic absorption overlapping the Ce^{3+} absorption bands located below 300 nm. In our powders such an effect is certainly also present, and it seems to be even more profound and extending for larger spectral region, underlying even the 345 nm Ce^{3+} absorption band. Consequently, we suppose that, contrary to the ceramics, in our fine powders the heat-treatment in air may lead not only to incorporation of interstitial Oxygen within the surface layer of grains but it also causes a partial $Ce^{3+} \rightarrow Ce^{4+}$ oxidation. The latter would end up with generation of $O^{2-} \rightarrow Ce^{4+}$ charge transfer (CT) absorption which is expected to extend over near-UV and partially also in short wavelength visible part of spectrum. Then, the excitation energy around 345 nm would need to be shared into both Ce^{3+} and Ce^{4+} ions, while only the former would contribute to emission. At 450 nm such a competition for the incoming energy by Ce^{4+} would be either absent or much less profound as only a tail of the CT band could extent to that part of spectrum. The treatment in reducing atmosphere would thus convert the Ce^{4+} into Ce^{3+} and the competing absorption giving no contribution to luminescence would no longer affect the ratio of the 345 nm and 450 nm excitation bands. We believe it is a reasonable explanation. Unfortunately, taking a good quality absorption spectra of the powders was not possible. Nevertheless, we noted that the air-treated samples had slightly lighter, more pale color, which substantiates the above consideration and conclusion. Comparing positions of the excitation and emission bands for the

samples treated at different atmospheres we did not see any measureable change in their position, which differs from data reported for powders of YAG:Ce [13].

The photoluminescence decay curves measured at room temperature under 450 nm excitation for LuAG:Ce^{3+} powder treated at different atmospheres are shown in Fig. 6 together with the trace recorded for a raw, untreated powder. All heat-treated samples gave traces of very similar course and the curves could be easily fitted with 2-exponential function is given as follows:

$$I = A + B_1 \exp(-t/\tau_1) + B_2 \exp(-t/\tau_2), \quad (1)$$

where I stands for intensity at time t, and τ_1 and τ_2 are the decay times. The derived values of the decay times were almost identical for all their specimens: $\tau_1 = 23$–24 ns and $\tau_2 = 75$–80 ns. Their relative contributions were also similar with the shorter component comprising about 25% of the emitted light. Note, that the longer component has value similar to single crystals (~60–70 ns) [7,14]. These numbers may imply that about 50% of Ce^{3+} ions incorporated into the LuAG host suffer from a kind of luminescence quenching. The slightly elongated decay time of the second component, $\tau_2 = 75$–80 ns, compared to regular decay observed in single crystals may be explained by the variation of the effective refractive index for fine grains of our fine powders, whose effect

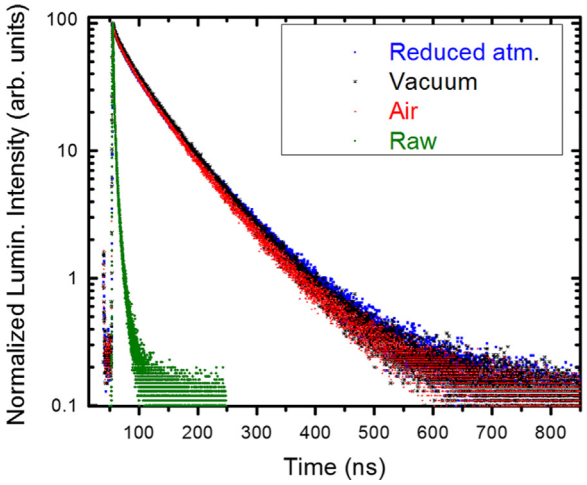

Fig. 6. RT photoluminescence decay traces of LuAG:Ce^{3+} powders heat-treated at 1150 °C at different atmospheres compared to the decay trace of a raw powder.

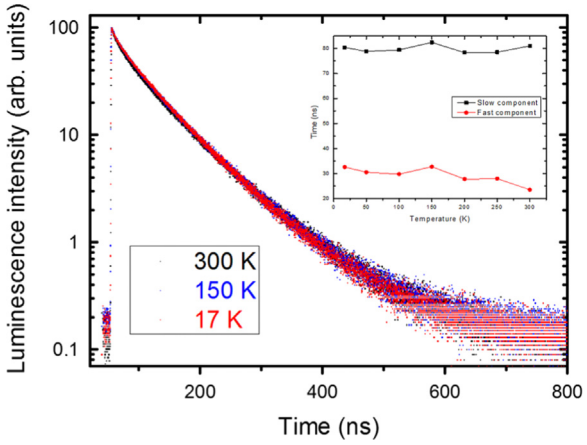

Fig. 7. Photoluminescence decay traces of LuAG:Ce^{3+} powders annealed at N_2–H_2 atmosphere taken at different temperatures in the range of 17–300 K. The inset shows the variation of the decay times of slow and fast components with temperature.

was reported and discussed in the literature in the past [15–20]. The decay trace of the raw powder made at 500 °C is also shown in Fig. 6. It is obvious that without the additional heat-treatment the luminescence of LuAG:Ce powder is strongly quenched, and reasonable fit could be done only with three exponential approach and the derived decay times were $\tau_1 = 1.1$ ns, $\tau_2 = 4.6$ ns and $\tau_3 = 19$ ns, among which the latter had only negligible contribution. The average decay time was calculated to reach ~2 ns. This value shows how significant quenching of luminescence is at work in the raw powders. Thus, although the LuAG:Ce powders may be indeed fabricated at extremely low temperatures of 450–550 °C getting reasonably efficient luminescence with only moderate quenching requires additional heat-treatment at 1150 °C.

Fig. 7 shows the dependence of the photoluminescence decays of LuAG:Ce^{3+} annealed at N_2–H_2 atmosphere at three selected temperatures in the range of 17–300 K. The variation of the two decay time constants with temperature is depicted as the inset of Fig. 7. Clearly, the decay curves are almost not affected by the temperature, indicating that there is not any significant temperature-driven luminescence quenching up to 300 K. This further means that the short component seen in the decays of the powders heat-treated at 1150 °C (see Fig. 6) is an intrinsic property of the fine LuAG:Ce powder rather and may be seen as an inherent prevailing property of the Ce^{3+} ions located in the vicinity of the grains surface. Some indication that Ce^{3+} surface ions has different luminescence kinetics was reported for YAG:Ce sintered ceramics. Yet, in the large grains of that ceramics, it was observed only for excitation with γ-rays [12]. Nevertheless, it seems that this is the highly developed surface with expected higher population of defects compared to the grains cores where all the quenching takes place.

4. Conclusions

In the present study the synthesis of LuAG:x% Ce ($x = 1$–5) nanocrystalline phosphor by the molten salts method with two different eutectic mixtures was described. Powder XRDs proved that the materials were crystalline already after preparation at 450–550 °C, and their morphology seen with SEM was similar and got not affected by heat-treatment at 1150 °C. Some separation of CeO_2 was proved for higher Ce concentrations and was anticipated to take place also for low Ce concentrations. The photoluminescence properties and the decays kinetics under 450 nm excitation were analyzed at various temperatures. Variations of relative intensities of the two main excitation bands at 340 nm and 450 nm were shown to mirror the changes reported by Robbins in YAG:Ce. Post-fabrication heat-treatment was shown to strongly enhance the luminescence efficiency by reduced quenching of the emission, as seen by changes in its decay time. The photoluminescence decay traces under 450 nm follow 2-exponential function with the fast and slow components of $\tau_1 = 23$–24 ns and $\tau_2 = 75$–80 ns being firmly constant in the 17–300 K range of temperatures.

Acknowledgments

The authors express their appreciations to Dr. Joanna Cybińska for her help and assistance in measurements of decay traces. Financial support of EC Marie Curie Initial Training Network LUMINET project No. 316906 (European Network on Luminescent Materials) is gratefully acknowledged.

References

[1] Y. Zorenko, J.A. Mares, R. Kucerkova, V. Gorbenko, V. Savchyn, T. Voznyak, M. Nikl, A. Beitlerova, K. Jurek, J. Phys. D: Appl. Phys. 42 (2009) 075501.
[2] M. Nikl, Meas. Sci. Technol. 17 (2006) R37.

[3] J. Tous, M. Horvath, L. Pına, K. Blazek, B. Sopko, Nucl. Instrum. Methods Phys. Res. A 591 (2008) 264.
[4] M. Nikl, E. Mihokova, J.A. Mares, A. Vedda, M. Martini, K. Neyezchleb, K. Blazek, Phys. Status solidi 181 (2000) R10.
[5] A.A. Setlur, A.M. Srivastava, Opt. Mater. 29 (2007) 1647.
[6] M. Nikl, E. Mihokova, J. Pejchal, A. Vedda, Y.u. Zorenko, K. Nejezchleb, Phys. Status Solidi (b) 242 (14) (2005) R119.
[7] Y.u. Zorenko, V. Gorbenko, A. Voloshinovskii, G. Stryganyuk, V. Mikhailin, V. Kolobanov, D. Spassky, M. Nikl, K. Blazek, Phys. Status Solidi (a) 202 (6) (2005) 1113.
[8] E. Zych, A. Walasek, J. Trojan-Piegza, A. Kossek, L. Kępiński, Radiat. Meas. 42 (4–5) (2007) 894.
[9] W. Zhao, C. Mancini, D. Amans, G. Boulon, T. Epicier, Y. Min, H. Yagi, T. Yanagitani, T. Yanagida, A. Yoshikawa, Jpn. J. Appl. Phys. 49 (2010) 022602.
[10] R.D. Shannon, C.T. Prewitt, Acta Cryst. B25 (1969) 925.
[11] D.J. Robbins, J. Electrochem. Soc. 126 (9) (1979) 1550.
[12] E. Zych, C. Brecher, A.J. Wojtowicz, H. Lingertat, J. Lumin. 75 (1997) 193.
[13] E. Zych, A. Walasek, A. Szemik-Hojniak, J. Alloy. Compd. 451 (2008) 582.
[14] M. Nikl, A. Vedda, M. Fasoli, I. Fontana, V.V. Laguta, E. Mihokova, J. Pejchal, J. Rosa, K. Nejezchleb, Phys. Rev. B 76 (2007) 195121.
[15] R.S. Meltzer, S.P. Feofilov, B. Tissue, H.B. Yuan, Phys. Rev. B 60 (1999) R14012.
[16] J.C. Boyer, F. Vetrone, J.A. Capobianco, A. Speghini, M. Bettinelli, J. Phys. Chem. B 108 (52) (2004) 20137.
[17] C. de Mello Donega, M. Bode, A. Meijerink, Phys. Rev. B 74 (2006) 085320.
[18] S.F. Wuister, C. de Mello Donega, A. Meijerink, J. Chem. Phys. 121 (2004) 4310.
[19] H.P. Christensen, D.R. Gabbe, H.P. Jensen, Phys. Rev. B 25 (1982) 1467.
[20] R.S. Meltzer, W.M. Yen, H. Zheng, S.P. Feofilov, M.J. Dejneka, B.M. Tissue, H.B. Yuan, J. Lumin. 94 (2001) 221.